Extraction of lakes from an IfSAR DSM and a GIS-based analysis of drainage potential, Western Arctic Coastal Plain of northern Alaska

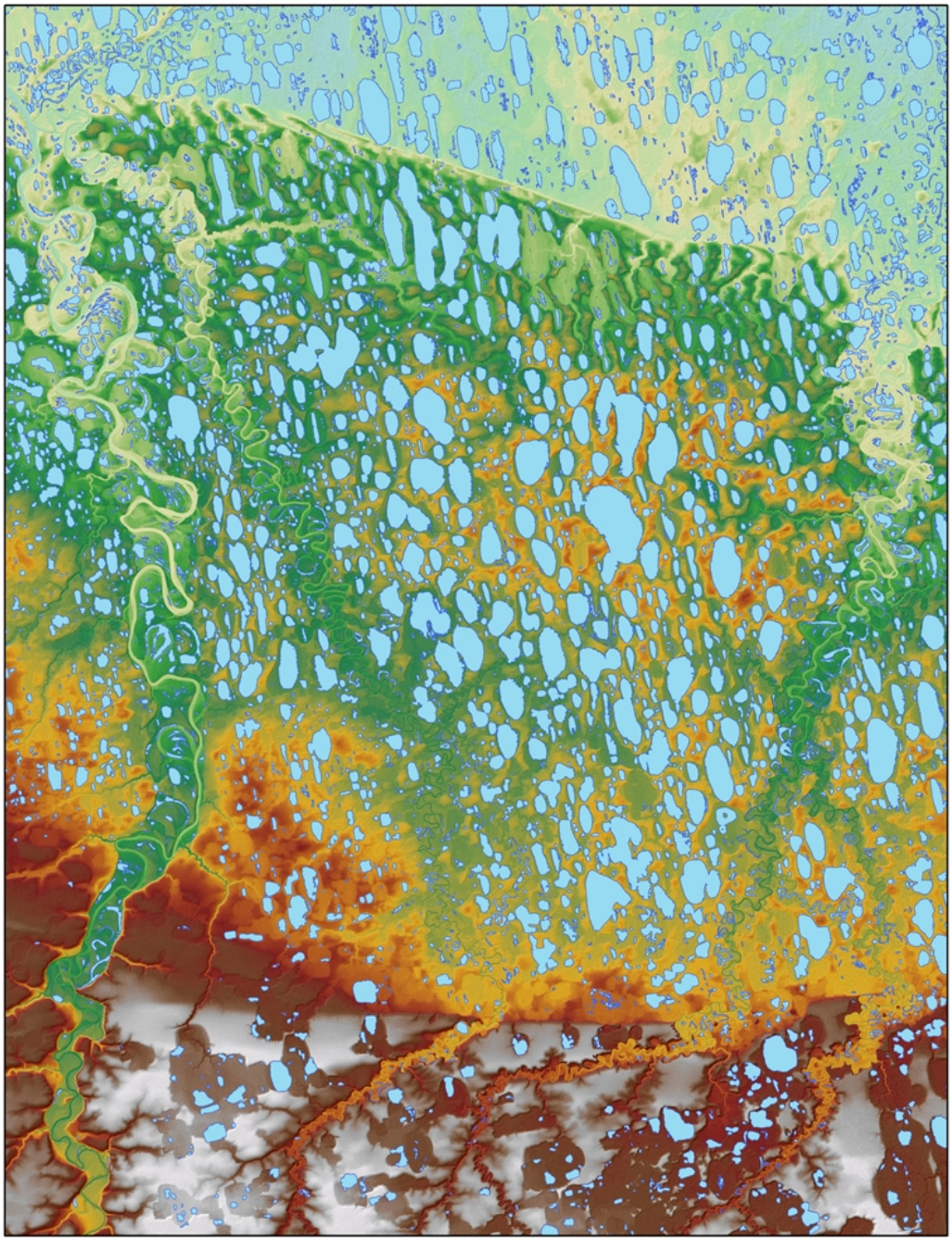

A report produced for the Arctic Landscape Conservation Cooperative

Title: Extraction of lakes from an IfSAR DSM and a GIS-based analysis of drainage potential, Western Arctic Coastal Plain of northern Alaska

Authors: Benjamin M. Jones[1] and Guido Grosse[2]

[1]Alaska Science Center, U.S. Geological Survey, Anchorage, AK
[2]Geophysical Institute, University of Alaska Fairbanks, Fairbanks, AK

Executive Summary

More than 35,000 lakes larger than 0.01 km^2 were extracted from an airborne interferometric synthetic aperture radar (IfSAR) derived digital surface model acquired between 2002 and 2006 for the Western Arctic Coastal Plain of northern Alaska. The IfSAR derived lake data layer provides an improvement over previously available datasets for the study area since it is more comprehensive and contemporary. Attributes assigned to the IfSAR-derived lake dataset include: area, lake elevation, elevation in 10, 25, 50, and 100 m buffers around a lake perimeter, the difference in elevation between the lake and these various buffers, whether a particular lake had a detectable drainage gradient (greater than 1.2 m), whether a particular lake intersected flowlines extracted from the National Hydrographic Dataset (NHD), potential susceptibility to drainage, NHD lake area, difference in area between the IfSAR and NHD lake data layers, whether a lake increased or decreased in area between these two datasets, the estimated difference in the radius of the lake based on a circle, an estimate of lake expansion rates over time, and likelihood of lake drainage as a result of lateral expansion by 2050 and 2100.

We identified 4,515 lakes (13%) as being susceptible to drainage based on a detectable drainage gradient within 100 m of the lake shoreline and no intersection with the NHD flowline data layer (a rough proxy for a currently closed-basin lake). Of these 4,515 lakes, 3,145 were classified as expanding, based on an increase in lake area between the NHD lakes data layer and IfSAR lakes data layer. When applying estimated expansion rates of these lakes to detectable drainage gradients in the IfSAR data, it appears that 8 may drain as a result of lake expansion by 2050 and 32 by 2100. However, these numbers should be viewed as a minimum and conservative estimate since only one of several potential drainage mechanisms were explored and a conservative gradient of 1.2 m was used. River channel migration, headward stream erosion, coastal erosion, ice-wedge degradation, top-down permafrost thaw, and human disturbance are also drainage mechanisms that could be incorporated into this dataset to provide more information on the timing associated with the drainage of lakes on the Western Arctic Coastal Plain of northern Alaska.

Suggested Citation: Jones, B.M. and G. Grosse, 2013, Extraction of lakes from an IfSAR DSM and a GIS-based analysis of drainage potential, Western Arctic Coastal Plain of northern Alaska, Report and data compiled for the Arctic Landscape Conservation Cooperative.

Products Delivered

1. IfSAR DSM mosaic of study area (5 m resolution)
    a. wacp_ifsar_dsm_5m_v2.ige
    b. wacp_ifsar_dsm_5m_v2.img
    c. wacp_ifsar_dsm_5m_v2.rrd
2. CIR orthophoto mosaic (5 m resolution)
    a. wacp_cir_mosaic_5m_study_area.ige
    b. wacp_cir_mosaic_5m_study_area.img
    c. wacp_cir_mosaic_5m_study_area.rrd
3. Polygon shapefile of extracted lakes larger than 0.01 km^2 with derived attributes
    a. wacp_lakes_v2.shp
    b. wacp_lakes_v2.shp.xml
    c. wacp_lakes_v2.dbf
    d. wacp_lakes_v2.sbn
    e. wacp_lakes_v2.sbx
    f. wacp_lakes_v2.shx
    g. wacp_lakes_v2.prj

Sample Map Showing Detected Lakes Potentially Susceptible to Drainage

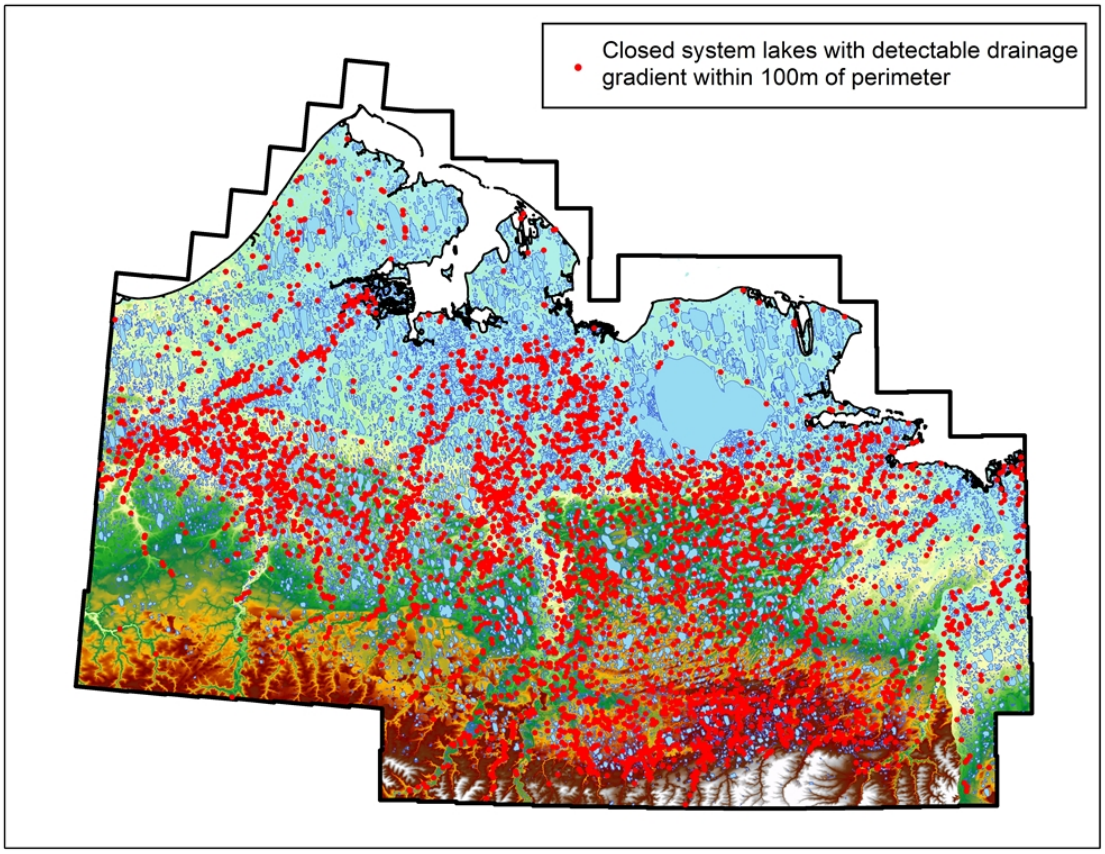

1. Introduction

Lakes on the Arctic Coastal Plain of northern Alaska provide essential habitat for many species of water birds and fish, but are vulnerable to the effects of climate change [*Martin et al.,* 2009]. Thus, it is critical for land and resource managers to be able to assess the potential vulnerability of any particular lake to changes in area and volume that may affect local and regional ecosystem characteristics. The vulnerability of an individual lake to drainage is dependent on ice content and ice distribution in the surrounding permafrost, lake characteristics (bathymetry, shore configuration, watershed and lake water balance), the existence of a topographic gradient, and external factors (climate, nearby erosional features such as streams, coasts, other lakes). Common mechanisms that may lead to lake drainage in the study area include ice-wedge degradation, headward stream erosion, river channel migration, coastal erosion, human disturbance, as well as expansion of a lake towards a drainage gradient [*Hopkins*, 1949; *Mackay*, 1988; *Brewer et al.*, 1993; *Hinkel et al.*, 2007; *Marsh et al.*, 2009; *Jones et al.,* 2011; *Grosse et al.*, 2013]. These mechanisms are in contrast to what one may find in thinner, discontinuous permafrost regions where internal drainage of thermokarst lakes has been documented as a talik (thawed zone) beneath a lake eventually penetrates the permafrost, allowing for drainage subterraneously [*Hopkins*, 1949; *Yoshikawa and Hinzman*, 2003].

Lakes have likely been forming and subsequently draining in the study area since the beginning of the Holocene (Figure 1). Lake extent may be as high as 20% for some Arctic lowland regions and an additional 50% may be comprised of drained lake basins [*Hinkel et al.,* 2003; *Grosse et al.,* 2005; *Hinkel et al.* 2005]. It is this matrix of active

lakes, drained lake basins, and remnant uplands that creates such diverse and unique wildlife habitats. Various studies have attempted to reconstruct the Holocene history of lake drainage events for various regions by assessing vegetative and geomorphic succession as well as post drainage peat accumulation [*Hinkel et al.*, 2003; *Jorgenson and Shur,* 2007*Jones et al.,* 2012; *Regmi et al.*, 2012]. Other studies have used remotely sensed image time series to assess lake drainage and determine landscape-scale drainage rates. *Mackay* [1988] found that between 1950 and 1986 roughly 65 lakes had drained completely or partially, yielding a drainage rate of ~1.8 lakes/yr for the Tuktoyaktuk Peninsula, Northwest Territories, Canada. *Hinkel et al.*, [2007] analyzed lakes larger than 10 ha for the western Arctic Coastal Plain of northern Alaska (34,000 km^2) and found that 50 lakes drained (> 25% reduction in surface area) between ca. 1975 and ca. 2000, and also found a drainage rate of ~2 lakes/yr. *Marsh et al.* [2009] provided estimates of lake drainage events from the Mackenzie Delta region by looking at three time periods, 1950 to 1973, 1973 to 1985, and 1985 to 2000 and found a reduction in the drainage rate of thermokarst lakes in the region, from 1.13 to 0.93 to 0.33 lakes/yr in each time period, respectively. However, for the Cape Espenberg lowland on the northern Seward Peninsula, *Jones et al.* [2011] found a fairly consistent drainage rate of 2.2 to 2.3 lakes/yr between two time periods (1950 to 1978 and 1978 to 2007). While these retrospective studies yield interesting results and provide useful information for long-term and short-term landscape dynamics, they do not provide readily useful information to land and resource managers striving to plan for the impacts of climate change. Thus, an analysis that attempts to provide spatially explicit information regarding the potential drainage of a particular lake would improve our capacity to link land cover mapping to

habitat models for migratory birds and fish in arctic Alaska, and thus predict habitat changes under varying climate scenarios and management regimes.

With advances in terrain mapping over the last several decades, high-resolution Digital Surface Models (DSM) have been acquired over relatively large regions in northern Alaska. Through analysis of these models, delineation of landscape drainage gradients is possible. By analyzing individual lakes and determining marginal drainage gradients it may be possible to develop a spatially explicit model framework that identifies potential lake drainage events across the landscape. This type of analysis could serve as one of the foundations for identifying the appropriate means and methods by which future habitat distribution can be identified and species distribution modeled in a geospatial environment. We have developed a spatially explicit data layer that identifies lakes that are potentially susceptible to drainage based on landscape drainage gradients. We have focused on a ~45,000 km^2 region of the western Arctic Coastal Plain, including portions of the National Petroleum Reserve –Alaska, an area-of-interest dictated by the availability of high resolution airborne Interferometric Synthetic Aperture Radar (IfSAR) derived DSM.

2. Study Area

Our study area extent was defined by the availability of an airborne Interferometric Synthetic Aperture Radar (IfSAR) derived digital surface model for the western Arctic Coastal Plain of northern Alaska (Figure 2). The data cover an area of approximately 45,000 km^2 and were acquired between 2002 and 2006 in a joint effort by the BLM, USGS, and NSF (Figure 3). The study area is part of the Arctic Coastal Plain of northern

Alaska, which is the second-largest lake district in the state [*Arp and Jones*, 2009], providing essential breeding, molting, and migratory stopover habitat for millions of migratory water birds, including 3 species of loons, and 20 species of large waterfowl (ducks, geese, and swans). Notable among these species are the Yellow-billed Loon, which is currently a candidate for listing under the Endangered Species Act, and Spectacled and Steller's eiders, both listed as "threatened." North Slope lakes also provide habitat for a variety of resident and anadromous fish, including least cisco, round whitefish, broad whitefish, lake trout, arctic char, arctic grayling, and ninespine stickleback. Lakes that are connected to stream systems are particularly important for fish, as are deep lakes (> 2 m) that provide over wintering habitat. North Slope lakes also provide a source of liquid water for communities and industry.

3. Extraction of lakes from the IfSAR DSM

A total of 312 IfSAR-derived digital surface model (DSM) tiles were merged to create a seamless mosaic for the 45,000 km^2 study area (Figure 2). As a result of "hydro-flattening" by the vendor during raw data processing, calculation of a slope derivative layer provides an initial approximation of water bodies for the study area. Thus, the slope derivative layer was used to extract all surface water features for the study domain. However, this technique for extracting waterbodies from the DSM inherently underestimates the entire perimeter of a water body by 1 pixel since the water body edge pixel always represents a non-zero slope. To account for this underestimation in lake area, the expand feature in ArcGIS® was used to automatically extend the perimeter of

every water body by 1 pixel. This binary raster file (water and non-water pixels) was then exported as a polygon vector for cleanup and analysis.

All features within 100 m of the study domain edge were removed from the dataset to prevent the inclusion of artificial drainage gradients associated with no data (0 m elevation) pixels. Next, all non-lake polygons were manually removed from the dataset by overlying the polygon layer on the CIR orthophoto mosaic and using a scale of 1:24,000. Once lakes had been isolated in the polygon data layer this was converted back to a 5 m resolution raster file for further editing. During this phase, the performance of the IfSAR extracted lake layer was assessed using the CIR orthophoto mosaic. In instances where there was an apparent discrepancy in the lake surface area between the two datasets the perimeter of the lake polygon was manually adjusted to match that of the CIR photos in raster space using the Arcscan tool in ArcMap®. This technique retained the raster grid network resolution (5 m) for depicting surface water area. After this step was complete, the binary raster lake layer was converted back to a polygon vector layer and compared to the initial estimate of lake surface area for the region (Figure 4). This resulted in the manual correction of 3,085 lakes or 9% of the lake population. This exercise also provided an indirect accuracy assessment by indicating that 91% of the lakes were accurately retrieved using the automated approach.

4. IfSAR-derived lake characteristics

Processing of the IfSAR-derived lake layer resulted in 35,283 lakes larger than 0.01 km^2 that cover an area of 7,737 km^2. Thus, lakes cover 17% of the study region. The mean lake size is 0.2 km^2 and the largest lake in the study region is Teshekpuk Lake (840 km^2). There are 13,777 lakes located between 0 to 15 meters above sea level (masl)

with a mean lake size of 0.27 km^2. There are 15,949 lakes located between 15 and 50 masl that roughly corresponds to the stabilized Pleistocene sand sheet and there is an interesting intermediate peak from 15 to 22 masl that corresponds to a geomorphic unit that likely corresponds to paleo coastal deposits from an interglacial period (see Jorgenson and Grunblatt, 2013). The mean lake size between 15 and 50 masl is 0.20 km^2. There are 5,557 lakes located between 50 and 140 masl. Lakes in this elevation category are located primarily in the northern foothills province. The mean lake area between 50 and 143 masl is 0.16 km^2. Thus, as the elevation increases in the study area mean lake area declines; whereas the number of lakes initially increases before declining.

5. Comparison to other available lake datasets

Comparing the IfSAR lake data layer with two statewide products, Alaskan Lake Database Mapped from Landsat Images [Sheng, 2012] and the U.S. Geological Survey National Hydrography Dataset [NHD, 2012], shows the importance of this newly created lake dataset. The minimum mapping unit used by Sheng [2012] was 0.1 km^2 and the data were derived from 30 m resolution Landsat data acquired between 1999 and 2002. Selecting lakes > 0.1 km^2 from our dataset shows that the Sheng dataset underestimates the number of lakes by 14% and lake area by 7% for lakes of minimum size of 0.1 km^2. If we compare all lakes in our dataset, greater than 0.01 km^2, to the Sheng [2012] dataset these discrepancies in lake number and area increase to underestimates of 130% and 17%, respectively. Comparing the IfSAR lake data to the more comprehensive NHD dataset, the number and area associated with lakes larger than 0.01 km^2 are within 0.25% and 1.2%, respectively. And given the history of the NHD dataset being compiled from

aerial photography acquired between 1955 and the 1980s, some of this difference may result from lake drainage events, lake formation events, differences in water level, seasonality, or methodologies use to extract the lake layers. Thus, the IfSAR derived lake data layer provides an improvement over previously available datasets for the study area since it is more comprehensive and contemporary. In addition, the derivation of the lake data layer from the IfSAR DSM data alleviate geolocation issues inherent in the NHD data and allow for direct comparisons and extraction of topographic information.

6. Lake Drainage Gradients

The ability to detect lake-based drainage gradients with the IfSAR DSM was assessed by comparing surface elevations of several overlapping tile edges (Figure 3 and Table 1). These showed a range in standard deviation of elevation between overlapping IfSAR tiles from 0.0 to 0.6 m. Thus, we decided to choose a height difference of 1.2 m (twice the maximum standard deviation) to represent a detectable drainage gradient adjacent to a lake feature. This value is also in-line with the field verified estimates of the vertical accuracy of the datasets around Barrow [Manley et al., 2005] and the stated vertical RMSE of the DSM data [Intermap, 2010].

By assessing several lakes that drained in the study area between the mid-1970s and early 2000s (*Hinkel et al.,* 2007) as well as between the NHD lake dataset and the IfSAR dataset, it appeared the drainage gullies were typically less than 100 m in length. Thus, lakes that were identified as having a detectable drainage gradient within the 100 m buffer were categorized as being susceptible to drainage. In order to identify lakes with a detectable drainage gradient a series of buffers (10, 25, 50, and 100 m) were used to

compare elevation of the lake surface to the surrounding terrain. There are 120 lakes with a detectable drainage gradient (> 1.2 m) within 10 m, 442 lakes within 25 m, 1,640 within 50 m, and 5,024 within 100 m of a lake. In order to refine this categorization further and account for open and closed basin lakes, the NHD Flowline data layer was used. Lakes that intersected the flowline layer were considered to not be susceptible to drainage since they likely have an outflow stream. Thus, lakes with a detectable drainage gradient within 100 m of their shoreline that did not intersect the flowline layer were classified as susceptible to drainage over some unspecified time frame (Figure 5). This totaled 4,515 lakes covering an area of 413 km^2 or 13% of the total lakes and 5.3% of the total lake surface area in the study region.

7. Estimating drainage based on lake expansion

In order to provide a potential estimate for the timing associated with lake drainage candidates we focused on one potential drainage mechanism, expansion of a lake towards a drainage gradient. Since not all lakes in the study region are expanding, the IfSAR lake data layer was compared to the NHD lake data layer to identify lakes that appeared to increase in size between the two datasets. There are 23,673 lakes with a surface area larger in the IfSAR compared to the NHD. These lakes were designated as potential expanding lakes and the change in radius of the polygon between the datasets was approximated based on a circle. Since the NHD lake data layer has a varied history of updates we assessed the NHD lake polygons relative to the original topographic digital raster graphics for the region that were based on mid-1950s imagery. It was apparent that nearly every quadrangle had been updated since the 1950s and most likely with aerial

photography from the late-1970s and early-1980s (AHAP program). Thus, in order to compare how well this approximation of lake expansion would perform we contrasted the change in radius for 10 lakes for which detailed measurements of lake expansion were conducted based on 1979 and 2002 aerial photography [Arp et al., 2011]. Comparing these two metrics shows good overall agreement, with an R^2 of 0.7 (Figure 6 and Table 2). The two outliers represented lakes with complex geometry or coalesced basins. Thus, we used this relationship as a first order approximation of lake expansion rates in our study area and applied the linear regression to the change in radius data. These estimated expansion rates were then compared to the buffer bins to determine the number of lakes likely to cross over a lake drainage gradient threshold by the year 2050 and 2100. These estimates and results indicate that 8 lakes are estimated to drain as a result of lake expansion toward a detectable drainage gradient by the year 2050 and 32 lakes are estimated to drain as a result of lake expansion toward a detectable drainage gradient by the year 2100. This would equate to a drainage rate of roughly 0.3 lakes per year when considering this drainage mechanism. However, this number should be viewed as a minimum as expanding lakes may drain prior to reaching the drainage gradient threshold and that there are several other drainage mechanisms operating on the landscape. In addition, this estimate does not factor in projected increases in air and permafrost temperature for the region and their connection to lake drainage potential. Nor does it account for a contagion effect whereby drainage in one lake increases the drainage gradient for surrounding waterbodies.

8. Implications

Information derived from the lake drainage gradient and potential drainage event dataset could be used to conduct detailed species-specific studies to determine the "winners" and "losers" associated with lake drainage on the landscape (Figure 7). A series of lakes with a high potential for drainage could be selected to monitor physical as well as biological processes leading up to and then following drainage. This type of data collection effort would provide detailed information on what may happen on the landscape-scale given future projections of reduced lake extent in the Arctic and increased wetland sedge habitat. The information in the drainage dataset is also of potential interest for subsistence users and industry as sites are selected for hunting and fishing cabins and drill site pads, respectively.

9. Conclusion

More than 35,000 lakes larger than 0.01 km^2 were extracted from an airborne interferometric synthetic aperture radar (IfSAR) derived digital surface model acquired between 2002 and 2006 for the Western Arctic Coastal Plain of northern Alaska. This lake data layer is an improvement over previously available lake data layers for the study region since it is more comprehensive and contemporary. There are 4,515 lakes identified as being susceptible to drainage based on a detectable drainage gradient (greater than 1.2 m) within 100 m of the lake shoreline and no intersection with the NHD flowline data layer (a proxy for a closed-basin lake). Of these 4,515 lakes, 3,145 were identified as an expanding lake based on an increase in lake area when comparing the IfSAR lake data layer to the NHD lake data layer. When applying estimated expansion

rates of these lakes to detectable drainage gradients in the IfSAR data, it appears that 8 may drain as a result of lake expansion by 2050 and 32 by 2100. River channel migration, headward stream erosion, coastal erosion, ice-wedge degradation, top-down permafrost thaw, and human disturbance are also drainage mechanisms that could be incorporated into this dataset to provide more information on the timing associated with the drainage of lakes on the Western Arctic Coastal Plain of northern Alaska.

Acknowledgments

Any use of trade, product, or firm names is for descriptive purposes only and does not imply endorsement by the U.S. Government.

Literature Cited

Arp, C. D., & Jones, B. M. (2009). Geography of Alaska lake districts: Identification, description, and analysis of lake-rich regions of a diverse and dynamic state. U. S. Geological Survey.

Arp, C. D., Jones, B. M., Urban, F. E., & Grosse, G. (2011). Hydrogeomorphic processes of thermokarst lakes with grounded-ice and floating-ice regimes on the Arctic coastal plain, Alaska. *Hydrological Processes*, *25*(15), 2422-2438.

Brewer, M. C., Carter, L. D., & Glenn, R. (1993, July). Sudden drainage of a thaw lake on the Alaskan Arctic coastal plain. In Proceedings of the Sixth International Conference on Permafrost. South China Univ. of Technology Press (pp. 48-53).

Grosse, G., Schirrmeister, L., Kunitsky, V. V., & Hubberten, H. W. (2005). The use of CORONA images in remote sensing of periglacial geomorphology: an illustration from the NE Siberian coast. *Permafrost and Periglacial Processes*, *16*(2), 163-172.

Grosse, G., B. Jones, and C. Arp (2013), Thermokarst Lakes, Drainage, and Drained Basins. In: John F. Shroder (Editor-inchief), Giardino, R., and J. Harbor (Volume Editors). Treatise on Geomorphology, Vol 8, Glacial and Periglacial Geomorphology, San Diego: Academic Press; p. 325-353.

Hinkel, K. M., Eisner, W. R., Bockheim, J. G., Nelson, F. E., Peterson, K. M., & Dai, X. (2003). Spatial extent, age, and carbon stocks in drained thaw lake basins on the Barrow Peninsula, Alaska. *Arctic, Antarctic, and Alpine Research*, *35*(3), 291-300.

Hinkel, K. M., Frohn, R. C., Nelson, F. E., Eisner, W. R., & Beck, R. A. (2005). Morphometric and spatial analysis of thaw lakes and drained thaw lake basins in the western Arctic Coastal Plain, Alaska. *Permafrost and Periglacial Processes*, *16*(4), 327-341.

Hinkel, K. M., Jones, B. M., Eisner, W. R., Cuomo, C. J., Beck, R. A., & Frohn, R. (2007). Methods to assess natural and anthropogenic thaw lake drainage on the western Arctic coastal plain of northern Alaska. *Journal of Geophysical Research: Earth Surface (2003–2012)*, *112*(F2).

Hopkins, D. M. (1949). Thaw lakes and thaw sinks in the Imuruk Lake area, Seward Peninsula, Alaska. *The Journal of Geology*, 119-131.

Intermap (2010), Product Handbook and Quick Start Guide, Standard Edition. Intermap, p. v 4.4.

Jones, B. M., Grosse, G., Arp, C. D., Jones, M. C., Walter Anthony, K. M., & Romanovsky, V. E. (2011). Modern thermokarst lake dynamics in the continuous permafrost zone, northern Seward Peninsula, Alaska. *Journal of Geophysical Research: Biogeosciences (2005–2012)*, *116*(G2).

Jones, M. C., Grosse, G., Jones, B. M., & Walter Anthony, K. (2012). Peat accumulation in drained thermokarst lake basins in continuous, ice-rich permafrost, northern Seward Peninsula, Alaska. *Journal of Geophysical Research: Biogeosciences (2005–2012)*, *117*(G2).

Jorgenson, M. T., and Y. Shur (2007), Evolution of lakes and basins in northern Alaska and discussion of the thaw lake cycle, J. Geophys. Res., 112, F02S17, doi:10.1029/2006JF000531.

Jorgenson, M. T., and J. Grunblatt (2013), Landscape-level ecological mapping of northern Alaska and field site photography, Report prepared for the Arctic Landscape Conservation Cooperative. [Available at http://arcticlcc.org/assets/products/ALCC2011-06/reports/NorthernAK_Landscape_Mappping_Field_Photos_Final_RPT.pdf].

Mackay, J. R. (1988). Catastrophic lake drainage, Tuktoyaktuk Peninsula area, District of Mackenzie. *Current Research, Part D, Geological Survey of Canada, Paper*, *88*, 83-90.

Manley, W. F., L. R. Lestak, C. E. Tweedie, and J. A. Maslanik. 2005. *High-resolution radar imagery, digital elevation models, and related GIS layers for Barrow, Alaska, USA*. Boulder, CO: National Snow and Ice Data Center. DVD.

Marsh, P., Russell, M., Pohl, S., Haywood, H., & Onclin, C. (2009). Changes in thaw lake drainage in the Western Canadian Arctic from 1950 to 2000. *Hydrological Processes*, *23*(1), 145-158.

Martin, Philip D., Jennifer L. Jenkins, F. Jeffrey Adams, M. Torre Jorgenson, Angela C. Matz, David C. Payer, Patricia E. Reynolds, Amy C. Tidwell, and James R. Zelenak. 2009. Wildlife Response to Environmental Arctic Change: Predicting Future Habitats of Arctic Alaska. Report of the Wildlife Response to Environmental Arctic Change (WildREACH): Predicting Future Habitats of Arctic Alaska Workshop, 17-18 November 2008. Fairbanks, Alaska: U.S. Fish and Wildlife Service. 138 pages.

National Hydrography Database (2012), http://nhd.usgs.gov/index.html.

Regmi, P., Grosse, G., Jones, M. C., Jones, B. M., & Anthony, K. W. (2012). Characterizing post-drainage succession in thermokarst lake basins on the Seward Peninsula, Alaska with TerraSAR-X backscatter and Landsat-based NDVI data. *Remote Sensing*, *4*(12), 3741-3765.

Sheng, Y. (2012). Alaskan Lake Database Mapped from Landsat Images. NCAR/UCAR/EOL, http://data.eol.ucar.edu/codiac/dss/id=106.346.

Yoshikawa, K., & Hinzman, L. D. (2003). Shrinking thermokarst ponds and groundwater dynamics in discontinuous permafrost near Council, Alaska. *Permafrost and Periglacial Processes*, *14*(2), 151-160.

Tables

Table 1. IfSAR DSM quality check by comparing the elevation values along the edge of nine overlapping tiles used to create the mosaic. Our threshold of 1.2 m for detectable drainage gradients is based on approximately twice the maximum standard deviation evident in the comparison of overlapping DSM tiles.

Tile Comparison	Standard Deviation (m)
umid3se vs. umic3ne	0.12
ikrc5ne vs. ikpc4nw	0.31
mera1sw vs. lord1nw	0.24
mera4sw vs. lord4nw	0.00
tesa2nw vs. tesa2ne	0.00
mera1ne vs. tesa5nw	0.58
tesd1sw vs. tesd1se	0.00
merd3se vs. merd3ne	0.47
bara3sw vs bara3se	0.51

Table 2. Comparison between measured lake expansion rates from 1979 and 2002 aerial photography (Arp et al. 2011) and an approximated change in radius for the same lakes based on comparison between the NHD and IfSAR lake polygon layers. Radius estimate based on a circle that encompasses the entire lake.

Lake ID	Measured Expansion Rates	Change in Radius
2568	1.8	17.08
2571	1.5	19.38
4704	1.2	15.64
2857	1.1	13.02
3784	1.1	13
4273	0.9	12.8
5808	0.7	17.2
3822	0.7	10.06
3838	0.5	5.94
2562	0.4	7.54
3360	0.2	4.78

Figures

Figure 1. Formation and drainage of lakes in the study region is a natural process that has been reshaping the landscape for about 10,000 years.

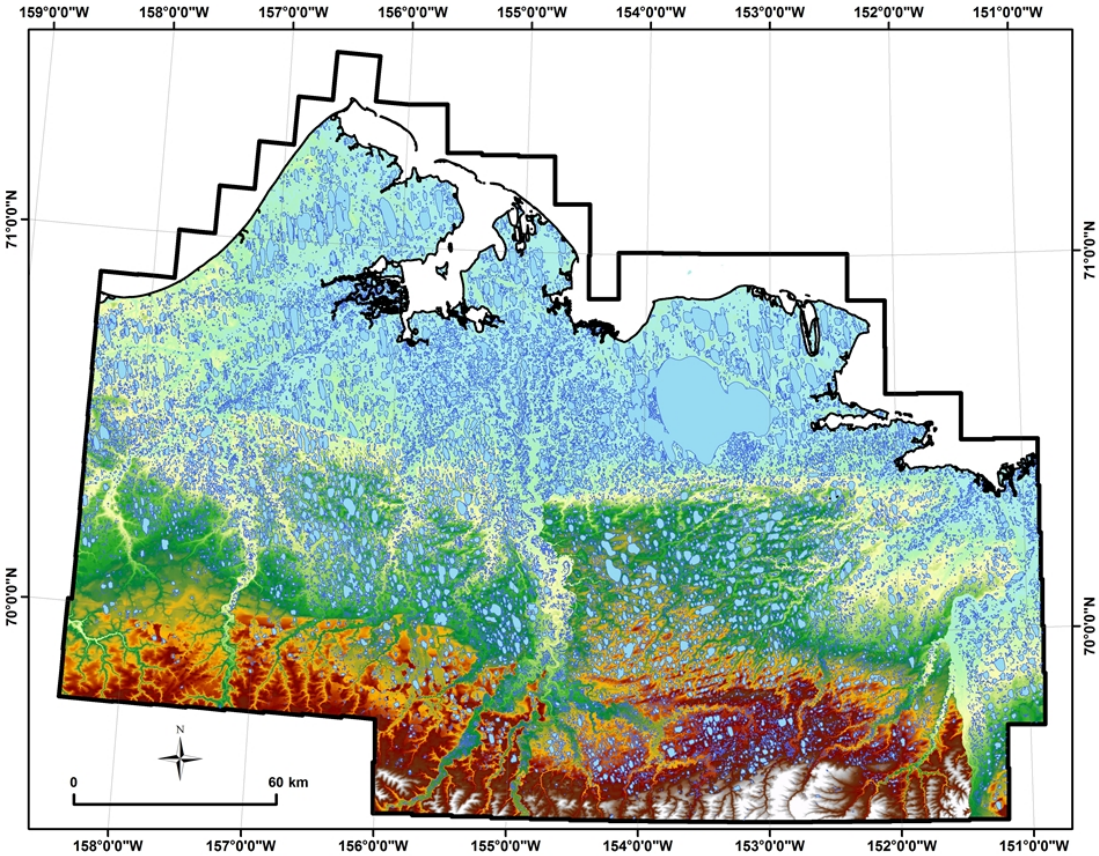

Figure 2. IfSAR digital surface model for the study area and extracted lakes as blue polygons.

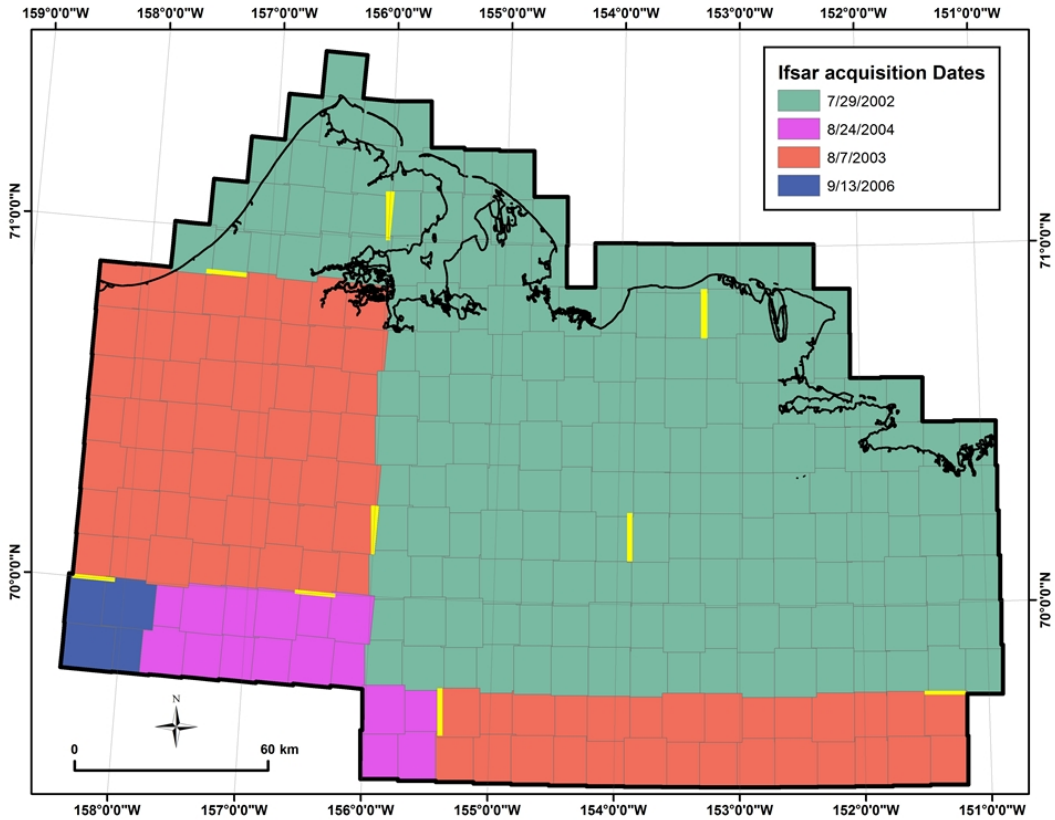

Figure 3. Acquistion dates of the IfSAR data used to make the DSM mosaic for the study area. The yellow rectangles indicate overlapping tiles that were used to determine the ability of the DSM to detect drainage gradients.

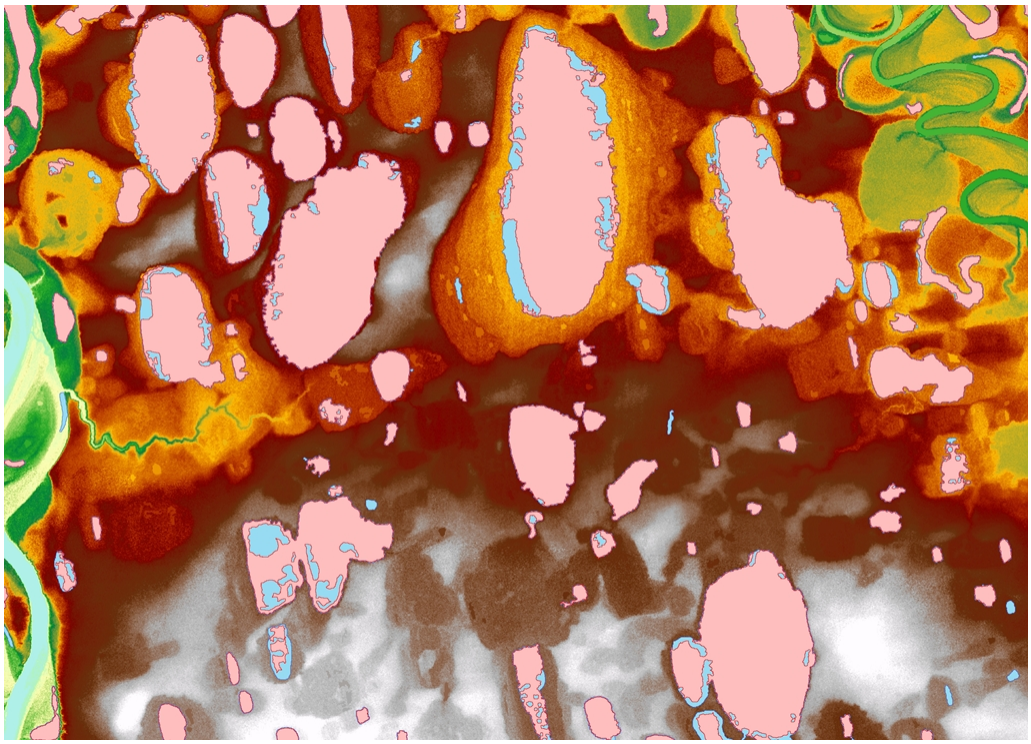

Figure 4. Comparison between automated and manually adjusted lake datasets. The pink polygons show the automated classification and the underlying blue polygons show the manually corrected lake dataset. Manual corrections were based on comparison with CIR orthophotography. This resulted in a manual adjustment of 9% of the 35,000 lakes.

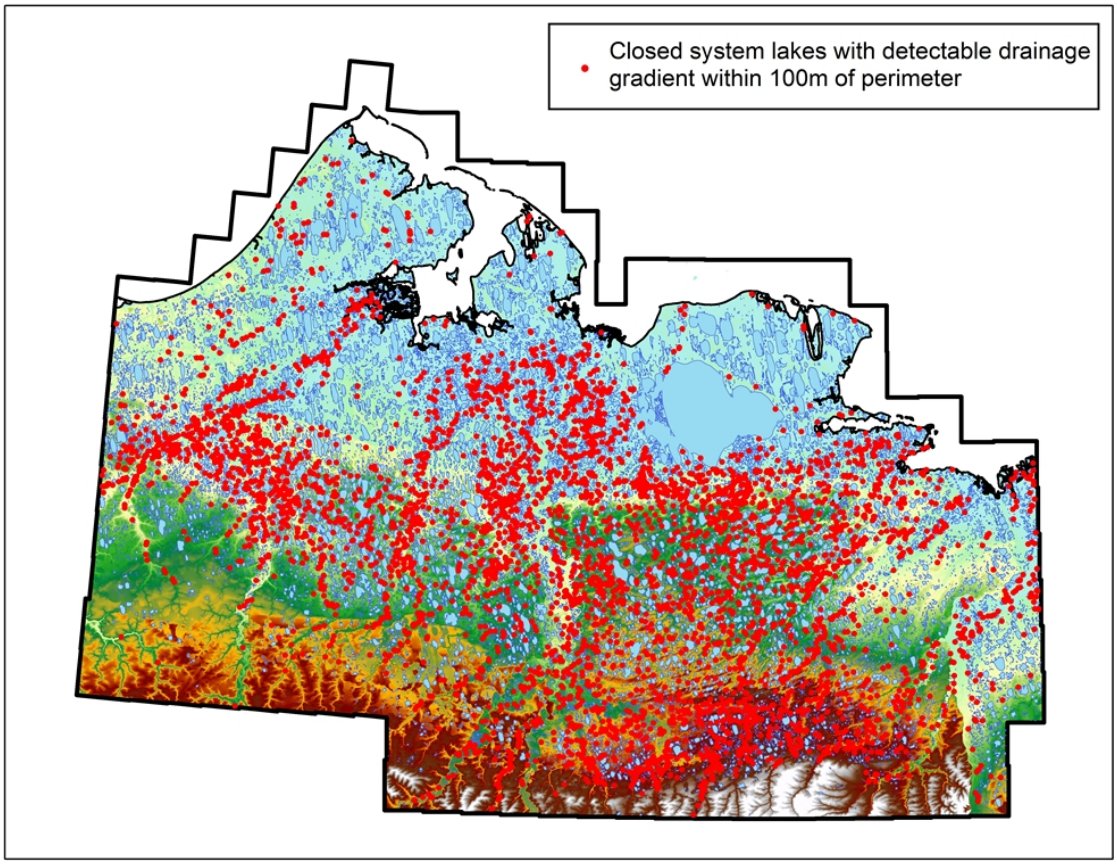

Figure 5. Closed system lakes (no intersection with NHD flowline layer) with a detectable drainage gradient (exceeding 1.2 m) within 100 m of the lake perimeter.

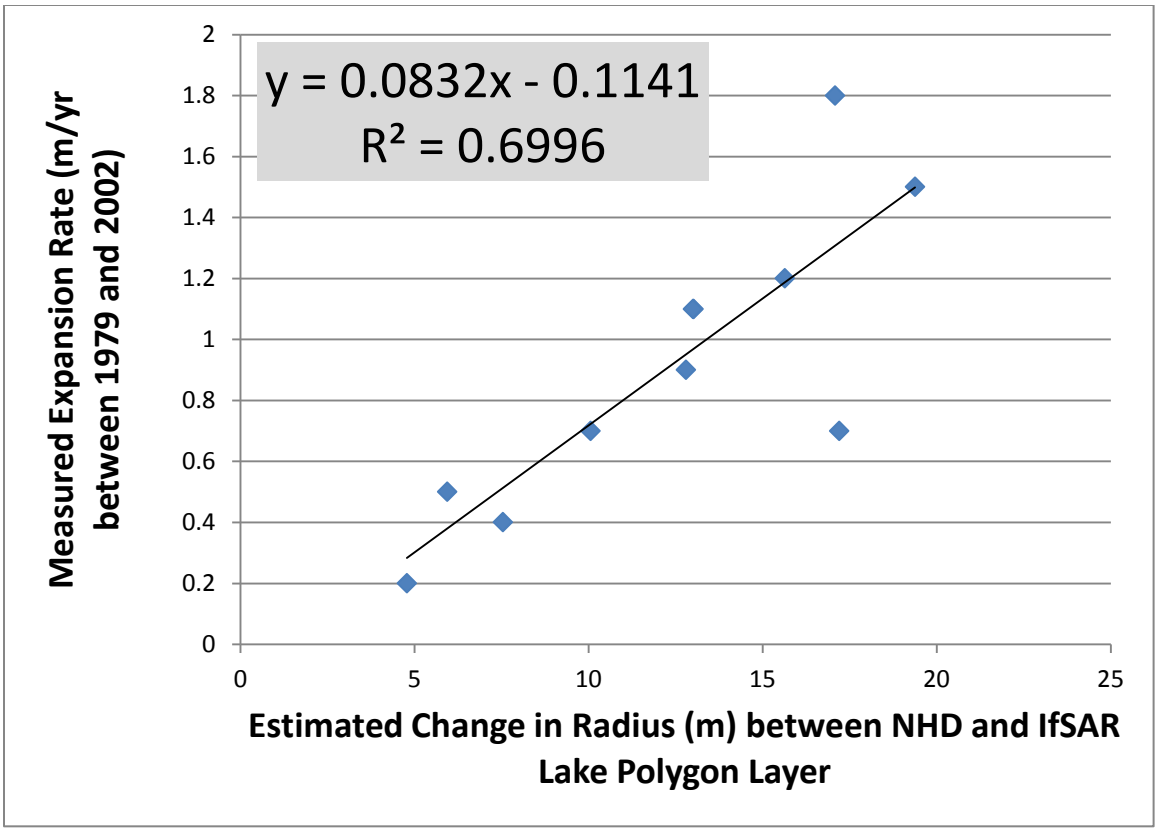

Figure 6. Comparison between measured lake expansion rates from 1979 and 2002 aerial photography [Arp et al. 2011] and an approximated change in radius for the same lakes based on comparison between the NHD and IfSAR lake polygon layers. Radius estimate based on a circle. The linear regression equation was used to estimate the expansion rate of lakes that increased in surface area between the last NHD update and the IfSAR data. Outliers indicate complex lake geometry.

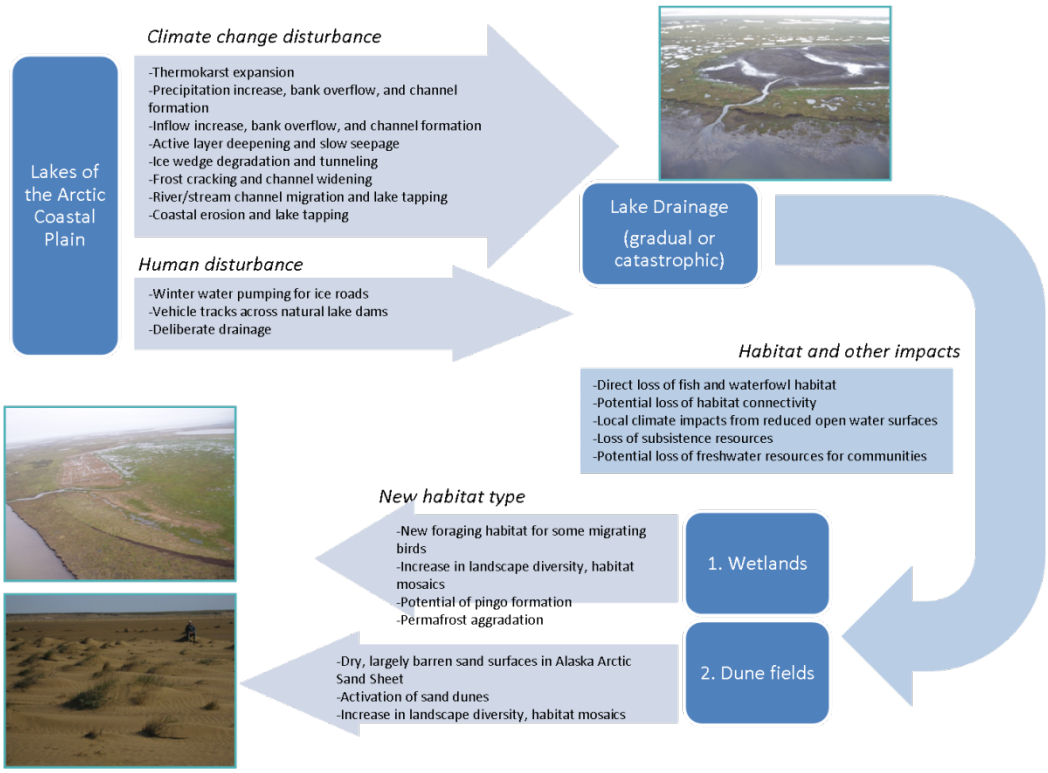

Figure 7. Conceptual schematic of linkages between physical processes and projected changes in available habitat.

Appendix 1

WACP_lakes_v2 (shapefile attributes):

- **FID** – ESRI default id for polygon
- **Shape** – Describes whether feature is point, line, or polygon
- **ID** – Unique ID for each lake derived from the IfSAR DSM
- **Area_sq_km** – The area of a lake polygon derived from the IfSAR data in square kilometers
- **Lake_hgt_m** – The minimum DSM elevation value for a given polygon
- **10m_hgt_m** – The minimum DSM elevation value for a 10 m buffer surrounding each lake polygon feature
- **25m_hgt_m** – The minimum DSM elevation value for a 25 m buffer surrounding each lake polygon feature
- **50m_hgt_m** – The minimum DSM elevation value for a 50 m buffer surrounding each lake polygon feature
- **100m_hgt_m** – The minimum DSM elevation value for a 100 m buffer surrounding each lake polygon feature
- **10m_diff** – The difference in minimum elevation between the lake surface and the 10 m buffer
- **25m_diff** – The difference in minimum elevation between the lake surface and the 25 m buffer
- **50m_diff** – The difference in minimum elevation between the lake surface and the 50 m buffer
- **100m_diff** – The difference in minimum elevation between the lake surface and the 100 m buffer
- **10m_drain** – Features coded 1 indicate a height difference between the lake surface and the 10 m buffer that exceeded 1.2 m. Features coded 0 indicate a height difference between the lake surface and the 10 m buffer that was less than 1.2 m
- **25m_drain** – Features coded 1 indicate a height difference between the lake surface and the 25 m buffer that exceeded 1.2 m. Features coded 0 indicate a height difference between the lake surface and the 25 m buffer that was less than 1.2 m
- **50m_drain** – Features coded 1 indicate a height difference between the lake surface and the 50 m buffer that exceeded 1.2 m. Features coded 0 indicate a height difference between the lake surface and the 50 m buffer that was less than 1.2 m
- **100m_drain** – Features coded 1 indicate a height difference between the lake surface and the 100 m buffer that exceeded 1.2 m. Features coded 0 indicate a height difference between the lake surface and the 100 m buffer that was less than 1.2 m
- **NHD_fl_int** – Features coded 1 indicate an intersection with the NHD flowline layer. Features coded 0 indicate that there was not an intersection with the NHD flowline layer

- **Susc_drain** – Features coded 1 indicate that there was a detectable drainage gradient within 100 m of the object perimeter and that there was no intersection with the NHD flowline layer. Features coded 0 indicate that there was no detectable drainage gradient within 100 m of the object perimeter and/or an intersection with with the NHD flowline layer
- **NHD_area** – This represents the area in square kilometer for a feature as defined from the NHD lake polygon layer. Values of 999999 indicate no value.
- **Area_diff** – This represents the difference in area in square meters between the NHD lake polygon layer and the IfSAR DSM lake polygon layer. Positive values indicate an increase in lake area and negative values indicate a decrease in lake area between the two datasets.
- **Expand_l** – Features coded 1 indicate an increase in lake area between the NHD lake polygon and IfSAR DSM lake polygon layers. Features coded 0 indicate a decrease in lake area between the NHD lake polygon and IfSAR DSM lake polygon layers. Features coded 999999 indicate no value.
- **Rad_diff** – This represents the estimate of radius change (based on a circle) in meters for lakes that increased in area between the NHD lake polygon and IfSAR DSM lake polygon layers. Features coded 999999 indicate a decrease in lake area or no value.
- **Est_exp_rt** – This represents an estimate of the lake expansion rate in m/yr for lakes that increased in area between the NHD lake polygon and IfSAR DSM lake polygon layers. This was based on the relation between measured lake expansion rates in aerial photography acquired in 1979 and 2002 and the estimated increase in lake radius based on comparison between the NHD and IfSAR polygon layers for feature IDs: 2562, 2568, 2571, 2857, 3360, 3784, 3822, 3838, 4273, 4704, and 5808. The equation used to derive this estimate was $y = 0.0832x-0.1141$ where y is the estimated expansion rate and x is the change in radius between the NHD and IfSAR lake polygon layers. Features coded 999999 indicate a decrease in lake area or no value.
- **Drain_2050** – Features coded 1 indicate lakes that will likely expand across a detectable drainage gradient by the year 2050. Features coded 0 indicate lakes that will likely not expand across a detectable drainage gradient by the year 2050.
- **Drain_2100** – Features coded 1 indicate lakes that will likely expand across a drainage gradient by the year 2100. Features coded 0 indicate lakes that will likely not expand across a detectable drainage gradient by the year 2100.